Available online at www.sciencedirect.com
SCIENCE DIRECT®
Pergamon
Cement and Concrete Research 34 (2004) 1859–1872
CEMENT AND CONCRETE RESEARCH

Coupled moisture—carbon dioxide–calcium transfer model for carbonation of concrete

B. Bary[a,*], A. Sellier[b,1]

[a]CEA Saclay, DEN/DPC/SCCME/LECBA, bât. 158, 91191 Gif/Yvette, France
[b]LMDC, Université P. Sabatier, 118 Route de Narbonne, 31062 Toulouse Cedex 4, France

Received 19 November 2002; accepted 29 January 2004

Abstract

The carbonation mechanisms of concrete are analyzed in this paper, accounting for evolutions of relative humidity in the porous material. The model is based on macroscopic mass balance equations for the water, the carbon dioxide contained in the gaseous phase and the calcium contained in the pore solution, which are supposed to completely define the problem of atmospheric carbonation in concrete. These equations govern the diffusion and permeation processes of the three variables: saturation degree, carbon dioxide partial pressure and calcium concentration in pore solution. By using an idealized description of the main hydrated products of the cement paste, the dissolution phenomenon can be regarded as depending only on the calcium concentration in the aqueous phase. The calcite formation and the hydrates dissolution are introduced in the mass balance as source terms and conduct to significant variations of the porosity. The mass balance equations are discretized in time and space in the one-dimensional case. The simulation of a concrete wall subjected to combined drying and accelerated carbon dioxide attack is then performed, and the results are analyzed and compared with experimental data in terms of carbonation depth.

Keywords: Carbonation; Degradation; Durability; Modeling; Numerical simulations

1. Introduction

The durability of cement-based materials is a topic of great concern in many fields of civil engineering. The prediction of the long-term behavior of concrete requires the identification and the analysis of the various deterioration mechanisms that will affect the structure. Among the numerous degradation causes, corrosion of the reinforcing steel induced by deleterious substances reaching the embedded bars is one of the most important [1,2]. This phenomenon is generally linked to a decrease of the concrete resistance to chemical attacks, which is widely related to the transport properties of the material; as a consequence, the ability of concrete to act as a barrier is no longer guaranteed. The reinforcing steel corrosion occurs theoretically when the three following basic conditions are encountered [1]: iron available in the metallic state, oxygen and moisture available for the cathode and a low electrical resistivity for the electron flow. In practice, external deleterious substances generally penetrate the concrete and reach the reinforcement bars, conducting to change the pore solution composition into aggressive conditions. The external substances are, for example, chloride ions contained in seawater and carbon dioxide contained in the atmosphere. Carbonation of concrete consists in the chemical reaction between the carbon dioxide present in the air and the calcium contained in the pore solution, in equilibrium with the hydration products of the cement. One of the main consequences of this phenomenon is the modification of the pH in the pore solution from a standard value between 12.5 and 13.5, to a value below 9 in the carbonated zones. This drop of the pH value leads to the destruction of the protective film (passive layer) that covers the reinforcing steel, so that the metallic iron becomes available and corrosion processes can carry on. As reported by several works, the quantities of water present in the pores are of great importance with regards to the carbonation phenomenon [1,3]. Indeed, although the carbonation reactions need

* Corresponding author. Tel.: +33-1-69-08-23-83; fax: +33-1-69-08-84-41.
E-mail addresses: bary@azurite.cea.fr (B. Bary), sellier@insa-tlse.fr (A. Sellier).
[1] Tel.: +33-5-61-55-67-04.

0008-8846/$ – see front matter © 2004 Elsevier Ltd. All rights reserved.
doi:10.1016/j.cemconres.2004.01.025

the presence of water for the cathode process, in high relative humidity conditions, the diffusion of both carbon dioxide and oxygen is reduced and even inhibited by the water filling the pores. The most suitable range of internal relative humidity for the carbonation of concrete seems to be 40% to 80% [1]; it can be noticed that values of relative humidity encountered in structural concrete are, in most cases, included within this range. However, a recent experimental investigation on several different concretes by Roy et al. [4] highlights a significant increase of the carbonation depth when the relative humidity passes from 84% to 92%.

Many works have been devoted to the analysis, modeling and simulation of the concrete carbonation processes in recent years [1,3–6]. The main purpose of these studies is, generally, to provide a theoretical approach capable of predicting the depth of carbonation in function of the time and of the external boundary conditions. The most sophisticated models consider the interaction between the following processes: diffusion of carbon dioxide, moisture and heat transfer, formation of calcium carbonate $CaCO_3$, dissolution of $Ca(OH)_2$ and diffusion of calcium in the pore solution [1,3]. Other approaches are based mainly on the mechanism of carbon dioxide diffusion through the porous material (widely linked to the saturation degree) and on its reaction with the calcium resulting from the dissolution of $Ca(OH)_2$ [5,6]. These studies concern mortars, but, as mentioned, the carbonation processes in such materials are similar with those occurring in concrete. Finally, some contributions give a simplified formulation, proportional to the square root of time, involving a coefficient depending on characteristics such as external carbon dioxide pressure and relative humidity, and constitution of the cement paste [7].

The object of this paper is to model the atmospheric carbonation processes of concrete when subjected to natural drying (that is, the material is considered as an unsaturated porous medium) in isothermal conditions. The extension to other external conditions (resaturation, accelerated carbonation experiments) is immediate due to the characteristics of the governing equations, which describe the mechanisms conducting to the carbonation phenomenon. The theoretical model is based on the mass balance equations for the water, the carbon dioxide flowing through the gaseous phase and the calcium concentration in the pore solution. These three species are assumed to completely define the state of the material with regard to the carbonation phenomenon. The dissolution of the main hydrates of the cement paste, as well as the formation of calcite, are introduced in the mass balance equations as source or sink terms; these two mechanisms lead to substantial variations of porosity and, consequently, to modifications of the transfer parameters for the three variables. The mass conservation equation for the water rests on the hypothesis that the transfer mechanism is mainly provoked by gradients of capillary pressure arising from the decrease of pore water content due to drying [8,9]. Moreover, a water source term takes into account the released water resulting from the dissolution of the hydrated products. The capillary pressure is directly related to the liquid phase (due to the low value of the gaseous phase pressure with respect to the liquid phase one), and the moisture transport is assumed to be controlled by this sole liquid phase, the contribution of the vapor transfer being neglected, as recently proposed by Mainguy et al. [9]. The dissolution of the main hydrates of the cement paste is supposed to be governed by the calcium concentration in the aqueous phase [10]. Moreover, the simplification consisting in assuming that the cement paste is composed of four main hydrates with regard to the progressive decalcification processes is adopted [10,11]. The three resulting partial differential equations are solved numerically in the one-dimensional case by application of a classical linearization procedure consisting in a time and space discretization. The parameters and functions introduced in the formulation are identified or adjusted on existing data and experiments, including accelerated carbonation tests.

In the first part of this paper the theoretical model is presented, then, an accelerated carbonation test is simulated and compared with experimental results. This comparison shows an acceptable agreement in terms of carbonation depth, and the numerical results highlight several phenomena of major importance regarding the carbonation process: the progressive filling of the porous space with calcite in the carbonated zone, which has a direct impact on the moisture, carbon dioxide and calcium transfers, and the quantity of solid calcium available for dissolution and calcite precipitation.

2. Governing equations

It is assumed in the ensuing development that the mean velocity of the solid phase is zero; that is, no deformation of the solid phase is taken into account. In this section, we are concerned with the establishment of the mass balance equations that govern the three state variables describing the phenomena under consideration. These variables are of different nature: one is a ionic specie (concentration of calcium ions in the pore solution which will be denoted C_a), another is chosen to be the water saturation degree of the connected porous space S_r (volume fraction of the porous space occupied by water), and the last is the partial pressure of carbon dioxide in the gaseous phase $p_{\bar{c}}$. However, the governing equations of this set of variables can be expressed in a general form. Consider a solute or constituent α subjected to transfer processes in the phase p (p could be the liquid or gaseous phase) and to chemical reactions; under the condition that the solid matrix undergoes no displacement, the mass balance equation for this solute then takes the form [12]:

$$\frac{\partial m_\alpha}{\partial t} + \mathrm{div}[w_\alpha] = S_\alpha, \tag{1}$$

with m_α as the total mass of α per unit volume of material, w_α as the mass flux of α and S_α as the rate of mass formation of α per unit volume of material. It should be noticed that S_α could be positive as well as negative, corresponding to a source or sink term, respectively. The general expression of the mass flux w_α is given by:

$$w_\alpha = \rho_\alpha \phi^{(p)} \dot{u}_\alpha = \rho_\alpha \phi^{(p)} (\dot{u}_\alpha^r + \dot{u}^{(p)}), \tag{2}$$

in which ρ_α is the mass of the solute α per unit volume of p phase, $\phi^{(p)}$ is the volume fraction of the phase p relative to the material, $\dot{u}_\alpha$ is the (absolute) velocity of α, and $\dot{u}_\alpha^r$ denotes the velocity of α relative to the phase p, whose mean velocity is $\dot{u}^{(p)}$. With these notations, the mass of α per unit volume of material can be written as $m_\alpha = \rho_\alpha \phi^{(p)}$. The general formulation of the mass balance equation can then be recast as:

$$\frac{\partial \rho_\alpha \phi^{(p)}}{\partial t} + \mathrm{div}[\rho_\alpha \phi^{(p)} \dot{u}^{(p)} + w_\alpha^r] = S_\alpha \tag{3}$$

where w_α^r denotes the macroscopic nonadvective (diffusive) flux of α due to molecular diffusion. It should be emphasized that the first term in the bracket defines the convective part of the flux (transport due to the movement of phase p). Moreover, the macroscopic dispersive part of the flux will be supposed to be included in w_α^r via the diffusion coefficient (see, for example, Ref. [2] for further details).

The mass balance for the phase p is easily deduced from Eq. (3) by replacing α with p and by considering that $\dot{u}_p^r = 0$, implying $w_p^r = 0$. Introducing Eq. (2), we then obtain:

$$\frac{\partial \rho_p \phi^{(p)}}{\partial t} + \mathrm{div}[w_p] = S_p. \tag{4}$$

The mass balance Eq. (3) can be expressed in another form, when p stands for the liquid phase, by making use of Eq. (4). In this case, by assuming ρ_p to be constant and invoking the identity $\mathrm{div}[\rho_\alpha \phi^{(p)} \dot{u}^{(p)}] = \mathrm{div}[(\rho_\alpha/\rho_p) w_p] = (\rho_\alpha/\rho_p)\,\mathrm{div}(w_p) + w_p\,\mathrm{grad}(\rho_\alpha/\rho_p)$, the insertion of Eq. (4) into Eq. (3) leads to:

$$\rho_p \phi^{(p)} \frac{\partial C}{\partial t} + \mathrm{div}[w_\alpha^r] + w_p\,\mathrm{grad}(C) = S_\alpha - C S_p \tag{5}$$

where $C = \rho_\alpha/\rho_p$ is the mass of α per unit mass of phase p. This expression is similar with, for example, the relation (Eq. (15)) established in Ref. [12]. Whatever the expression retained for the mass balance, some additional constitutive equations are required to complete the formulation. Indeed, conduction laws have to be introduced to define some relations between the mass fluxes and the state variables. In the ensuing developments, the preceding mass balance equation will be applied successively to the water, the carbon dioxide diffusing through the gaseous phase and the calcium concentration diffusing in the pore solution.

2.1. Mass conservation of water

Applying Eq. (4) for obtaining the expression of the mass conservation for the water (in which the subscript p is replaced by l), we get:

$$\frac{\partial \rho_l \phi S_r}{\partial t} = -\mathrm{div}[w_l] + S_l, \tag{6}$$

where, for convenience, we introduce the total porosity ϕ (or volume fraction of the porous space relative to the material) connected to the volume fraction occupied by the water phase by $\phi^{(l)} = \phi S_r$. We now are concerned with detailing the expressions of the water flux w_l and the rate of water formation S_l. In this work, we make the assumption that the main phenomenon conducting to moisture transport is due only to the liquid flowing through the connected porosity [9]; as a consequence, the mass exchange between liquid water and vapor is neglected. Under this condition, S_l is proposed in the following form:

$$\begin{aligned} S_l &= k_{sl}(S_r) M_{H_2O} \frac{\partial \omega_{ls}(C_a)}{\partial t} \\ &= k_{sl}(S_r) M_{H_2O} \omega'_{ls}(C_a) \frac{\partial C_a}{\partial t}, \text{ with } \omega'_{ls} = \frac{d\omega_{ls}(C_a)}{dC_a}. \end{aligned} \tag{7}$$

This relation expresses the water mass supply resulting from the progressive dissolution of the main hydrated products retained in the description of the cement paste. The term $\omega_{ls}(C_a)$ denotes the concentration of water involved in these solid phases per unit volume of material, which releases in the porous space when decalcification occurs. This degradation process is supposed to be controlled by the sole calcium concentration C_a in the pore solution [10–13] (see the next section for further details). M_{H_2O} is the molar mass of water, and the function $k_{sl}(S_r)$ describes, at the macroscopic scale, the influence of the saturation degree drop on the chemical reaction processes (which can be attributed, to a certain extent, to both the reduction of water and of contact surfaces between the water and the hydrated products). It affects the decalcification phenomena by acting on the mass of water and calcium released in the corresponding mass balance equations. For the sake of simplicity, and due to the lack of information, this function is chosen as the one proposed by Bazant and Najjar [14]:

$$k_{sl}(S_r) = \frac{1}{[1 + 625(1 - S_r)^4]}. \tag{8}$$

The mass flux of water is classically expressed via the Darcy conduction law:

$$w_l = -\frac{K(\phi)\rho_l}{\eta} k_{rl}(S_r)\,\mathrm{grad}(p_l) \tag{9}$$

where p_l and $K(\phi)$ are the pressure of the liquid phase and the intrinsic permeability coefficient, respectively; η denotes the

viscosity of the water supposed to be constant. The macroscopic function $k_{rl}(S_r)$ affects $K(\phi)$ by accounting for the variations of saturation degree due to moisture transfer and porosity variation. The following form based on a formulation proposed in Ref. [15] and adopted by Baroghel-Bouny et al. [8], among others, is retained:

$$k_{rl}(S_r) = \sqrt{S_r}[1 - (1 - S_r^b)^{1b}]^2, \tag{10}$$

where b is a real scalar, set to 1.65 for the numerical applications. We assume that the intrinsic permeability coefficient depends on the total porosity by the following expression, drawn from Ref. [15]:

$$K(\phi) = K_0 \left(\frac{\phi}{\phi_0}\right)^3 \left(\frac{1-\phi_0}{1-\phi}\right)^2, \tag{11}$$

where K_0 denotes the intrinsic permeability, corresponding to the reference porosity ϕ_0. Assuming that the pressure of the gaseous phase is negligible with respect to the liquid one, we have $p_{cap} = p_m - p_l \approx -p_l$, with p_{cap} and p_m as the capillary and the gas mixture pressures, respectively. Invoking the Kelvin's law, which relates the pressure p_{cap} to the relative humidity h_r by:

$$p_{cap}(h_r) = -\rho_l \frac{RT}{M_v} \ln[h_r(S_r)], \tag{12}$$

and, under the hypothesis of the existence of the function $h_r(S_r)$ to be identified, Eq. (9) can be recast as:

$$w_l = \frac{K(\phi)\rho_l}{\eta} k_{rl}(S_r) p'_{cap}(h_r) h'_r(S_r) \mathrm{grad}(S_r). \tag{13}$$

In Eq. (12), M_v is the molar mass of the vapor, R and T stand for the ideal gas constant and temperature, respectively; $f'(x)$ denotes the derivative of f with respect to its unique argument x; that is, $f'(x) = \mathrm{d}f(x)/\mathrm{d}x$. In Eq. (13), use has been made of the identity $\mathrm{grad}[p_{cap}(h_r)] = p'_{cap}(h_r)\mathrm{grad}[h_r(S_r)] = p'_{cap}(h_r)h'_r(S_r)\mathrm{grad}(S_r)$.

To complete the formulation of the water mass balance (Eq. (6)), some additional equations defining the evolutions of the current porosity ϕ, which is strongly dependent on both the dissolution of the hydrated products and the calcite formation, have to be introduced. The general expression of ϕ is given by:

$$\phi = \phi_0 + V_d(t) - V_{cal}(t), \tag{14}$$

where $V_d(t)$ and $V_{cal}(t)$ are the current volume fractions of the dissolved hydrated products and the formed calcite, respectively, per unit volume of material. By denoting $\dot{N}_{cal}$ the molar rate of calcite formation per volume of pore solution (this term will be detailed below), the (local) volume rate of calcite formation per volume of material $\mathrm{d}V_{cal}/\mathrm{d}t$ takes the form:

$$\frac{\mathrm{d}V_{cal}(t)}{\mathrm{d}t} = \dot{V}_{cal}(t) = V_{CaCO_3} \phi S_r \dot{N}_{cal}, \tag{15}$$

in which V_{CaCO_3} is the molar volume of the calcite. Integrating this relation with time, we get:

$$V_{cal}(t) = V_{CaCO_3} \int_0^t \phi(\tau) S_r(\tau) \dot{N}_{cal}(\tau) \mathrm{d}\tau. \tag{16}$$

As indicated in the Introduction (see the next section for more explanations), the calcium concentration in pore solution C_a is assumed to govern the decalcification processes, at constant saturation degree. In the following, we denote $V_{dt}(C_a)$ as the volume fraction per unit volume of material of decalcified hydrated products at calcium concentration C_a and in saturated conditions (i.e., ideally $V_{dt}(0) = V_{dt_{MAX}}$ and $V_{dt}(C_{a_{MAX}}) = 0$, where $V_{dt_{MAX}}$ and $C_{a_{MAX}}$ stand for the total volume fraction of decalcified hydrated products and the calcium concentration in pore solution for the intact material, respectively). With these notations, the volume rate of dissolved hydrated products $\mathrm{d}V_d(t)/\mathrm{d}t$ reads:

$$\frac{\mathrm{d}V_d(t)}{\mathrm{d}t} = k_{sl}(S_r) \frac{\mathrm{d}V_{dt}(C_a)}{\mathrm{d}t} = k_{sl}(S_r) \frac{\mathrm{d}V_{dt}(C_a)}{\mathrm{d}C_a} \frac{\mathrm{d}C_a}{\mathrm{d}t}. \tag{17}$$

Integrating this relation with time or, equivalently, with the calcium concentration [for which the initial condition is given by $C_a(t=0) = C_{a0}$] leads to the following expression for $V_d(t)$:

$$V_d(t) = \int_{C_{a0}}^{C_a(t)} k_{sl}(S_r) \left[\frac{\mathrm{d}V_{dt}(C_a)}{\mathrm{d}C_a}\right] \mathrm{d}C_a = \int_{C_{a0}}^{C_a(t)} k_{sl}(S_r) \mathrm{d}V_{dt}. \tag{18}$$

Let us now detail the rate of calcite formation $\dot{N}_{cal}$ introduced in Eqs. (15) and (16). According to the hypothesis of chemical equilibrium adopted in this work, all chemical reactions are supposed to be instantaneous, so that at every time, each ionic specie present in pore solution is in equilibrium with the gaseous and solid species involved in the reactions. This assumption is considered to be realistic in the sense that the diffusion phenomena are slow relative to the rates of reactions and then play a crucial role regarding the kinetics of the processes. However, from a numerical viewpoint, the case of instantaneous reactions is not easy to deal with when solving the equations. For the sake of simplicity, and to give a physical meaning to our formulation, we suppose that the main reaction leading to calcite precipitation is $C_a^{2+} + CO_3^{2-} \rightarrow C_aCO_3$, and we adopt a first-order reaction law in calcium and in carbonate to approach the corresponding rate of calcite formation (see, for example, Ref. [16]). We propose to adapt this law to the variables of our system (i.e., to replace the concentration of carbonates by the partial pressure of carbon dioxide in gaseous phase $p_{\tilde{c}}$) and to correct it by the function $k_{gl}(S_r)$ to account for the saturation degree evolutions in the form:

$$\dot{N}_{cal} = \vartheta k_{gl}(S_r) p_{\tilde{c}} C_a, \tag{19}$$

where ϑ is the rate constant of the law to be experimentally determined. The function $k_{gl}(S_r)$ can be interpreted as a

reduction factor acting on the dissolution of the carbon dioxide from the gaseous phase into the water (gas–liquid transfer), in function of the saturation degree; it therefore strongly depends upon the contact surfaces between the gaseous and liquid phases. In the cases where $S_r = 0$ and 1, because the interfaces between gas and liquid do not exist any more, we necessarily have $k_{gl} = 0$. We propose the simplified normalized (ranging between 0 and 1), following expression for the function $k_{gl}(S_r)$:

$$k_{gl}(S_r) = \xi S_r^{\alpha}(1 - S_r^{\beta}), \text{ with } \xi = \left(\frac{\alpha}{\beta}\right)\left(\frac{\alpha}{\alpha+\beta}\right)^{-\frac{\alpha+\beta}{\alpha}}, \tag{20}$$

in which α and β are two positive parameters. The choice of $\alpha = \beta = 1.5$ results from the assumption of a maximum carbon dioxide transfer between the gaseous phase and the liquid one for a saturation degree centered around 60% (see Fig. 1); this choice is motivated by some experimental observations (see, for example, Ref. [17]). The rate constant ϑ is assessed by considering the expression of the reaction rate for the calcite formation proposed in Ref. [7] as $r_{CH} = HRTK_2[OH^-]_{eq}[CO_2]$, in which H is the Henry constant (34.510^{-5} mol/m^3/Pa), K_2 is the reaction rate between the carbon dioxide CO_2 and OH^- ($K_2 = 8.3$ m^3/mol/s), $[CO_2]$ is the molar concentration of CO_2 in the gaseous phase (proportional to the variable $p_{\bar{c}}$ introduced in Eq. (19)) and $[OH^-]_{eq}$ is the concentration of OH^- corresponding to the chemical equilibrium after the total dissolution of portlandite (43.2 mol/m^3). By comparing Eq. (19) and the relation giving r_{CH} (in which the above numerical values have been replaced), and with the concentration of C_a in Eq. (19) being assessed to 21 mol/m^3, in the case where the portlandite is totally dissolved (this value results from a calculation with the simplified chemical approach adopted in this study; see Section 3 for details), we obtain the value of $\vartheta = 0.123$ Pa^{-1}s^{-1}. It should be remarked here that this value for ϑ is not relevant relative to the chemical equilibrium hypothesis; indeed, for this case, the appropriate value is infinity, corresponding to instantaneous reactions. However, as outlined above, the phenomena are considered to be diffusion controlled and, thus, the influence of ϑ is secondary, providing that its value is sufficiently high for the condition of diffusion prevalence to be fulfilled. This point would deserve further investigations and some numerical verifications.

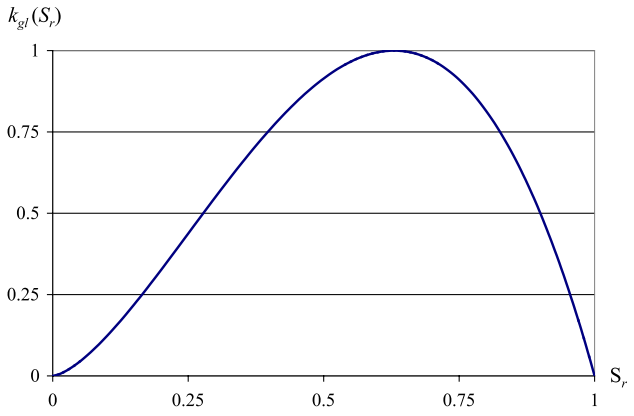

Fig. 1. Evolutions of the function $k_{gl}(S_r)$.

Finally, we propose to rearrange Eq. (6) of the mass balance for water by inserting the terms detailed previously. Invoking Eq. (14), the left-hand side of Eq. (6) can be expanded as:

$$\frac{\partial \rho_l \phi S_r}{\partial t} = \rho_l \phi \frac{\partial S_r}{\partial t} + \rho_l S_r \left[\frac{\partial V_d(t)}{\partial t} - \frac{\partial V_{cal}(t)}{\partial t}\right]. \tag{21}$$

By making use of Eqs. (15) and (17), the second term of this relation can be recast as:

$$\rho_l S_r \left[\frac{\partial V_d(t)}{\partial t} - \frac{\partial V_{cal}(t)}{\partial t}\right] = \rho_l S_r \left[k_{sl}(S_r)\frac{dV_{dt}(C_a)}{dC_a}\frac{\partial C_a}{\partial t} - V_{CaCO_3}\phi S_r \dot{N}_{cal}\right]. \tag{22}$$

Introducing these last two expressions, together with Eqs. (7) and (13), in Eq. (6), we obtain the following form for the mass conservation of the water:

$$\rho_l \phi \frac{\partial S_r}{\partial t} + \left[\rho_l S_r k_{sl}(S_r)\frac{dV_{dt}(C_a)}{dC_a} - k_{sl}(S_r)M_{H_2O}\omega'_{ls}(C_a)\right] \times \frac{\partial C_a}{\partial t} - \rho_l \phi (S_r)^2 V_{CaCO}\ \dot{N}_{cal} + \text{div}\left[\frac{K(\phi)\rho_l}{\eta} k_{rl}(S_r)p'_{cap}(h_r)h'_r(S_r)\text{grad}(S_r)\right] = 0. \tag{23}$$

2.2. Mass conservation of the carbon dioxide

The mass conservation of the carbon dioxide in the gaseous phase is expressed by applying the general mass balance Eq. (3), in which $\phi^{(p)}$, ρ_α, $\dot{u}^{(p)}$, w_α^r and S_α are replaced by $\phi(1 - S_r)$ (volume fraction of the gaseous phase), $\rho_{\bar{c}}$ (mass density of CO_2 in the gaseous phase), $\dot{u}^{(g)}$ (mean velocity of the gaseous phase), $w_{\bar{c}}$ (diffusive flux of CO_2 in the gaseous phase) and μ_{gl} (source term describing the dissolution rate of CO_2 into the liquid phase, which combines with calcium to form calcite), respectively. Then, we have:

$$\frac{\partial \phi(1 - S_r)\rho_{\bar{c}}}{\partial t} + \text{div}[\rho_{\bar{c}}\phi(1 - S_r)\dot{u}^{(g)} + w_{\bar{c}}] = -\mu_{gl}. \tag{24}$$

We now detail the different terms involved in Eq. (24). Under the assumption of an immediate reaction between the dissolved carbon dioxide and the calcium, μ_{gl} can be directly related to the molar formation rate of calcite $\dot{N}_{cal}$. Recalling that $\dot{N}_{cal}$ is defined per unit volume of pore

solution and that each mol of precipitated calcite requires 1 mol of calcium and one of carbonate (implying that the number of moles of calcium and carbonate needed to form any quantity of calcite is equal), the mass rate of CO_2 involved in calcite formation per unit volume of material is:

$$\mu_{gl} = M_{\bar{c}} \phi S_r \dot{N}_{cal}, \tag{25}$$

with $M_{\bar{c}}$ as the molar mass of carbon dioxide. The hypothesis formulated in the previous section concerning the homogeneity of the gas mixture pressure p_m within the material still holds. Consequently, the transport of CO_2 reduces to the only diffusion in the gaseous phase (the diffusion of CO_3^{2-} in the pore solution being neglected, as suggested in Ref. [18]). Moreover, as p_m is supposed to be constant in the material, the ensemble transfer of the gaseous phase due to gas pressure gradients is zero, and we have $u^{(g)} = 0$. Furthermore, we consider that this gaseous phase is composed of carbon dioxide and air, which form an ideal mixture of two ideal gases. The formulation of the diffusion law (Fick's law) requires, in a general case, a choice in the weights for expressing the average velocity of the mixture $u^{(g)}$ (the most common choices for these weights are the mass fractions or molar fractions; see for example, Ref. [19]). In our study, this average velocity is zero, and we adopt the form giving directly the diffusive mass flux of CO_2 as [19]:

$$w_{\bar{c}} = -f(\phi, S_r) D_{\bar{c}} \rho_m \mathrm{grad}(c_{\bar{c}}), \tag{26}$$

where $D_{\bar{c}}$ is the diffusion coefficient of CO_2 (which is the same as the one for the air, according to the binary mixture theory), $f(\phi,S_r)$ is the resistance factor describing the tortuosity effects and the variation of space offered to the gaseous constituents, ρ_m is the mass density of the gas mixture and $c_{\bar{c}} = \rho_{\bar{c}}/\rho_m$ denotes the mass fraction of CO_2 relative to the mixture. Invoking the ideal gas law for both the CO_2 and the air, expressed as $\rho_i = p_i M_i/(RT)$ for constituent i (i = m and $\bar{c}$), the diffusive mass flux $w_{\bar{c}}$ can be recast as:

$$w_{\bar{c}} = -f(\phi, S_r) D_{\bar{c}} \frac{M_{\bar{c}}}{RT} p_m \mathrm{grad}\left(\frac{p_{\bar{c}}}{p_m}\right). \tag{27}$$

Eq. (27) does not account for Knudsen and dispersion effects due to the heterogeneity of the velocity distribution at the microscopic scale. Because p_m is assumed to be constant, it can be reduced to:

$$w_{\bar{c}} = -f(\phi, S_r) D_{\bar{c}} \frac{M_{\bar{c}}}{RT} \mathrm{grad}(p_{\bar{c}}). \tag{28}$$

The coefficient $f(\phi,S_r)D_{\bar{c}}$ can be regarded as the macroscopic diffusion coefficient of the gaseous constituents through the porous material. Numerous expressions have been proposed by researchers for the reduction factor $f(\phi,S_r)$ involved in Eq. (27); we retain the one derived by Millington [20] for variably saturated porous media and used by several authors, among others [9,21]:

$$f(\phi, S_r) = \phi^{4/3}(1 - S_r)^{10/3}. \tag{29}$$

We now proceed to reformulate the mass balance Eq. (24) by introducing the terms defined in this section and the preceding one. We first recall that the CO_2 is considered as an ideal gas, which formally reads:

$$\rho_{\bar{c}} = \frac{M_{\bar{c}}}{RT} p_{\bar{c}}. \tag{30}$$

We then expand the first term of Eq. (24) in the form:

$$\frac{\partial \phi(1 - S_r)\rho_{\bar{c}}}{\partial t} = \frac{M_{\bar{c}}}{RT}\left\{(1 - S_r)p_{\bar{c}}\frac{\partial \phi}{\partial t} - p_{\bar{c}}\phi\frac{\partial S_r}{\partial t} + \phi(1 - S_r)\frac{\partial p_{\bar{c}}}{\partial t}\right\} \tag{31}$$

where use have been made of Eq. (30). Utilizing this result with the expression of $\partial\phi/\partial t$ established in Eq. (22), and introducing Eqs. (28) and (25) into Eq. (24), gives the following formulation for the mass conservation of the carbon dioxide in the gaseous phase, in which appears the time derivative of the variables defining the state of the system:

$$\begin{aligned}&(1 - S_r)p_{\bar{c}}k_{sl}(S_r)\frac{dV_{dt}(C_a)}{dC_a}\frac{\partial C_a}{\partial t} + \phi(1 - S_r)\frac{\partial p_{\bar{c}}}{\partial t}\\ &-\phi p_{\bar{c}}\frac{\partial S_r}{\partial t} + \phi S_r \dot{N}_{cal}[RT - (1 - S_r)p_{\bar{c}}V_{CaCO_3}]\\ &-\mathrm{div}[f(\phi, S_r)D_{\bar{c}}\mathrm{grad}p_{\bar{c}}] = 0.\end{aligned} \tag{32}$$

2.3. Mass conservation of the calcium in the pore solution

The mass balance equation for the calcium present in the pore solution is derived from Eq. (3), where the superscript p stands for the pore solution [then, $\phi^{(p)} = \phi S_r$] and ρ_α is replaced by the mass density of the calcium in pore solution ρ_a. Making use of the identity $\rho_a = M_a C_a$ with M_a as the molar mass of calcium, and dividing Eq. (3) by M_a we get:

$$\frac{\partial \phi S_r C_a}{\partial t} + \mathrm{div}\left[C_a\frac{w_l}{\rho_l} + w_a\right] = S_a, \tag{33}$$

where w_a is the diffusive flux of calcium in the pore solution, and S_a is the source term describing the molar rate of calcium exchange between the water and the other phases. As already mentioned, in Eq. (33), the first term in the bracket is the convective part of the flux and characterizes the calcium transport due to the movement of the water containing the solute C_a [2]. The second term in the bracket describes the flux of molecular diffusion of C_a in the water, and is expressed by the classical Fick's law:

$$w_a = -D_a(S_r, \phi)\mathrm{grad}C_a, \tag{34}$$

in which $D_a(S_r,\phi)$ is the effective (or global) diffusion coefficient of C_a through the porous material. The right-

hand side of Eq. (33) stands for the source (or sink) term governed by the decalcification and the calcite formation processes, and which leads to increase (or decrease) the calcium concentration in the liquid phase. By denoting $C_{aS}(C_a)$ the calcium concentration in the solid phase per unit volume of porous material, whose variations are supposed to be only dependent on C_a, and making use of the definition of the calcite formation rate $\dot{N}_{cal}$ and the function k_{sl}, the source term S_a introduced in Eq. (33) is given by

$$S_a = -k_{sl}\frac{dC_{aS}(C_a)}{dt} - \phi S_r \dot{N}_{cal}. \quad (35)$$

The first term in the right-hand side of Eq. (35) is the molar rate of calcium per unit volume of material released by the hydrated products when decalcifying; the second term is the molar rate of calcium implied in the calcite formation process, already defined in Eq. (25). Finally, the mass balance equation for the calcium in the liquid phase is expressed, in function of the time derivative of the state variables, in the following form:

$$\begin{aligned}&\left[\phi S_r + S_r C_a k_{sl}(S_r)\frac{dV_{dt}(C_a)}{dC_a} + k_{sl}(S_r)\frac{dC_{aS}(C_a)}{dC_a}\right]\frac{\partial C_a}{\partial t}\\ &+\phi C_a \frac{\partial S_r}{\partial t} + \phi S_r \dot{N}_{cal}[1 - S_r C_a V_{CaCO_3}]\\ &-\mathrm{div}\left[\frac{C_a K(\phi)}{\eta} k_{rl}(S_r) p'_{cap}(h_r) h'_r(S_r)\mathrm{grad}(S_r)\right.\\ &\left.+D_a(S_r,\phi)\mathrm{grad}(C_a)\right] = 0. \end{aligned} \quad (36)$$

This relation is obtained by expanding, as for the mass balance equations of water and CO_2, the first term of Eq. (33), and by introducing Eqs. (22) and (13), giving the expression of $\partial\phi/\partial t$ and w_l, respectively. The global diffusion coefficient of C_a depends both on the porosity and on the saturation degree and is assumed to take the following expression:

$$D_a(S_r,\phi) = k_{sl}(S_r) D_e(\phi), \quad (37)$$

where $k_{sl}(S_r)$ is defined by Eq. (8), and $D_e(\phi)$ is taken from Ref. [22]:

$$D_e = 2.3\ 10^{-13}\exp[9.95\phi(t)]. \quad (38)$$

3. Chemical description of the hydrated products

The aim of this section is to formulate the source (or sink) terms used in the three mass balance equations presented in Section 2. These terms are mainly dependent on the chemical composition of the hydrated cement paste and take into account both the chemical product quantities given by the chemical analyses of anhydrous cement and the chemical equilibrium conditions governing the dissolution and precipitation mechanisms.

3.1. Principles

Carbonation leads to a progressive decalcification of the hydrated cement paste. This decalcification occurs when the calcium concentration decreases in the pore water because of the calcium consumption induced by the carbonation reaction. The portlandite is first dissolved, followed by AFm, AFt and $C–S–H$, which are progressively decalcified in the function of the C_a decreasing in pore solution. The decalcification of cement paste has the three main following consequences: calcium release in the pore water, hydration water release in porosity and porosity volume modification.

As exposed in Section 2, these phenomena are taken into account in the mass balance equations governing the system by several terms, which are assessed by adopting a simplified chemical description of the hydrated cement paste. This description, proposed by Adenot [11] for the leaching modeling of cement paste, consists for an Ordinary Portland Cement (OPC), in assuming that the cement is initially hydrated in four main components:

- Portlandite (CH): $Ca(OH)_2$,
- CSH($C_a/S_i = 1.65$): $1.65CaO\ SiO_2\ 2.45H_20$,
- Monosulphate (AFm): $3CaO\ Al_2O_3\ CaSO_3\ 12H_2O$,
- Ettringite (AFt): $3CaO\ Al_2O_3\ 3CaSO_3\ 32H_2O$ or Hexahydrate (Hexa): $3Ca0\ Al_2O_3\ 6H_2O$.

The component quantities depend linearly upon the four main oxide component quantities present in the anhydrous cement. Adopting the following notation for mole number of oxide component per unit volume of cement paste, $SiO_2 = S$, $CaO = C$, $SO_3 = \bar{S}$, $2Al_2O_3 + 2Fe_2O_3 = A + F$, we can assess a theoretical composition of the completely hydrated cement paste by solving the following set of :

$$\begin{cases} C = CH + 1.65CSH + 4\mathrm{AFm} + 6\mathrm{AFt(or\ 3\ Hexa)} \\ S = CSH \\ A + F = 2\mathrm{AFt(or\ 2\ Hexa)} + 2\mathrm{AFm} \\ \bar{S} = 3\mathrm{AFt(or\ 0\ Hexa)} + \mathrm{AFm} \end{cases}. \quad (39)$$

3.2. Simplified chemical equilibrium

The calcium C_a and the carbonate CO_3 (for simplicity, the electric charge is omitted in the ionic specie notation when appearing in the text) present in the pore water are combined to form calcite, according to Eq. (40). The equilibrium condition in Eq. (41) is assumed to be fulfilled locally when carbonation process occurs (i.e., when CO_3 is nonzero in the pore solution), implying the

presence of calcite in the material, at least in small quantities.

$$C_a^{2+} + CO_3^{2-} \rightarrow C_aCO_3, \quad (40)$$

$$[C_a^{2+}][CO_3^{2-}] = 10^{-8.35}. \quad (41)$$

As previously stated, the ionic specie C_a is provided in the pore water by the dissolution of the hydrated products, whereas CO_3 results from the dissolution of carbon dioxide present in the gaseous phase. The chemical equilibrium equations governing the carbon dioxide dissolution used in our approach are taken from Ref. [23]. When carbonation occurs, the consumption of dissolved C_a leads to a decrease of C_a concentration in the pore water. First, this decrease is compensated by *CH* dissolution; after total dissolution of *CH*, C_a are taken from the Aft, AFm and *C–S–H* hydrated phases. In the case of leaching, Adenot [11] has shown that the decalcification mechanism can be described, for an idealized hydrated cement paste, by a chemical zoning characterized by the C_a ionic concentration in pore water. In our approach, the same basic description is adopted and completed by Eqs. (40) and (41) for reproducing a carbonation phenomenon. The idealized chemical zoning used for evaluating the ionic concentration of the main species involved in coupled decalcification and carbonation description is shown in Table 1. Both C_a and CO_2 pressure values defining the zone boundaries result from calculations of chemical equilibriums involving different solid phases, depending on the zone (see Ref. [11] for further details). In each zone, the evolutions in terms of molar content of the hydrated products undergoing decalcification (defining the decalcification rate) are supposed to be linear in the function of C_a, which varies between the boundary values of the zone. No alkali ions are considered in these calculations, and the ion strength correction model used is the well-known modified Davies law (see, for example, Ref. [24]). One of the most important aspects of the simplified Adenot approach resides in the discretization of the decalcification mechanisms for the *C–S–H*. Starting from this idea, we propose to model the progressive decalcification of the *C–S–H* phase, characterized by C_a/S_i ratios ranging from 1.65 for intact material to about 0.80 for a totally degraded one, by introducing four *C–S–H* with C_a/S_i ratios equal to 1.65, 1.45, 0.90 and 0.85.

Table 2
Expression of the source terms used in the mass balance equations in function of the calcium concentration in pore solution (mol/m^3)

C_a (mol/m^3)	$(dC_{aS})/(dC_a)$	ω'_{LS}	$10^6(dV_{dt})/(dC_a)$ (m^3/mol)
$C_a = 22.0$	0	0	0
$22.0 > C_a \geq 21.0$	(*CH*)/(22.0–21.0)	(*CH*)/(22.0–21.0)	(33.1*CH*)/(22.0–21.0)
$21.0 > C_a \geq 14.8$	(4 AFm + 0.2 *CSH*)/(21.0–14.8)	(12 AFm + 0.2 *CSH*)/(21.0–14.8)	(313 AFm)/(21.0–14.8)
$14.8 > C_a \geq 9.30$	[6 AFt (or 3 Hexa) + 0.55 *CSH*]/[14.8–9.30]	[32 AFt (or 6 Hexa) + 0.55 *CSH*]/[14.8–9.30]	[715 AFt (or 150 Hexa)]/[14.8–9.30]
$9.30 > C_a \geq 1.60$	(0.05 *CSH*)/(9.30–1.60)	(0.05 *CSH*)/(9.30–1.60)	0
$1.60 > C_a \geq 0.40$	(0.85 *CSH*)/(1.60–0.40)	(1.65 *CSH*)/(1.60–0.40)	0
$0.40 > C_a$	0	0	0

In Table 1, the Zone 0 represents the sound material and does not contain calcite; it is characterized by the C_a concentration equal to 22 mol/m^3. The *CH* is linearly dissolved in Zone 1 (where calcite appears at first), for which C_a varies from 22 to 21 mol/m^3. AFm is progressively dissolved in Zone 2, and *C–S–H* starts to decalcify (its C_a/S_i ratio passes linearly from 1.65 to 1.45). In Zone 3, Aft is totally decalcified, whereas the C_a/S_i ratio of *C–S–H* continues to decrease. In Zones 4 and 5, *C–S–H* progressively decalcifies and vanishes, and in Zone 6, where all C_a are combined in calcite, the material is considered as completely carbonated. One can remark, when regarding the Table 1 results, that as long as the C_a value remains high in pore water, the CO_2 pressure is close to zero, which means that the CO_2

Table 1
Idealized solid phase zoning used for ionic concentration assessment in pore water

Chemical zoning for carbonation process						
Zone 6	Zone 5	Zone 4	Zone 3	Zone 2	Zone 1	Zone 0
Solid phases						
Calcite	Calcite	Calcite	Calcite	Calcite	Calcite	
	C–S–H (0.85)	*C–S–H* (0.90)	*C–S–H* (1.45)	*C–S–H* (1.65)	*CH*	*CH*
		C–S–H (0.85)	*C–S–H* (0.90)	*C–S–H* (1.45)	*C–S–H* (1.65)	*C–S–H* (1.65)
			Aft	Aft	Aft	Aft
				Afm	Afm	Afm
Calculated calcium concentration in pore water (mol/m^3) and gas pressure (Pa)						
C_a	0–0.40	1.60	9.30	14.8	21.0	22.0
CO_2 partial pressure	32	1.80E − 06	2.90E − 09	9.10E − 10	2.40E − 10	

Table 3
Cement chemical composition CPA CEM I 52.5 R

(% mass)	
Fe_2O_3	2.38
Al_2O_3	5.19
CaO	64.02
SO_3	3.5
H_2O	2.23
SiO_2	19.81

cannot reach the intact zone with a high pressure value and, consequently, the consumption of C_a and CO_2 occurs on a very localized zone. This remark is in good agreement with usual experimental observations and with assumptions formulated in several simplified carbonation modeling proposed in the literature (see, for example, Ref. [3–7]).

3.3. Source terms

The assumptions concerning the solid phases present in each zone (and their decalcification occurring linearly in function of C_a), as represented in Table 1, allow to assess the calcium content in residual hydrated phases during carbonation process. Then, the source term of the calcium mass conservation equation, denoted as dC_{aS}/dC_a in Eq. (36), depends upon C_a by the linear relations expressed in Table 2 for each chemical zone. Starting from the molar volume of each solid phase present in a zone, we can assess the total dissolved volume in function of the calcium concentration, and, consequently, the term dV_{dt}/dC_a appearing in the conservation Eqs. (23), (32) and (36) can be estimated by the expressions given in Table 2. Furthermore, during carbonation process, the hydrated product dissolution leads to the release of hydration water in porosity, which modifies the degree of saturation and, consequently, the connectivity of the gaseous phase and the liquid phase network. This released water is taking into account in the mass conservation equation of water (Eq. (23)) by the term $\omega_{lS}'(C_a)$. To assess this term, we use the mole number of H_2O, given by the usual chemical composition of the hydrated products (i.e., 12 mol/mol of AFm, 32 mol for AFt, 1 mol for *CH*); for *C–S–H*, the H_2O mole number

Table 5
Composition of 1 l of cement paste

In mol/m^3 of cement paste				
C	S	$A+F$	$\bar{S}$	H_2O
14860	4290	1710	570	1610

n depends on the C_a/S_i ratio. We have adopted for n the expression given by Ref. [25]:

$$n = C_a/S_i + 0.80 \tag{42}$$

The expression of the term $\omega_{lS}'(C_a)$ obtained for each chemical zone is given in Table 2.

4. Numerical applications

The three partial differential Eqs. (23), (32) and (36) are solved numerically in the one-dimensional case. The source terms defined in Table 2, together with the function $h_r(S_r)$ introduced in Eq. (12), are given explicitly in the particular case of a CEM I concrete. The simulation of the behaviour of a concrete wall subjected to accelerated carbonation is then carried out, analyzed and confronted to experimental data.

4.1. Numerical procedure

The implementation of Eqs. (23), (32) and (36) in one dimension is obtained by applying a classical linearization procedure, which consists in discretizing these equations in both time and space domains, conducting to a system of three algebraic nonlinear equations for each time step. The nonlinearity results from the solution dependency of the coefficients involved in the governing equations. The space and time domains are discretized by using the classical finite–difference method (the unknowns are calculated at a discrete set of points disposed on a grid) and the θ-method, respectively. The latter is characterized by a linear approximation of the evolution of the unknowns within each time step, i.e., when denoting $\theta=(t-t_n)/(t_{n+1}-t_n)$, with $0\leq\theta\leq 1$, the evolutions of the state variable $X(t)$ within $[t_n,t_{n+1}]$ are defined by:

$$X(t) = (1-\theta)X(t_n) + \theta X(t_{n+1}). \tag{43}$$

In the numerical applications presented in the sequel, we have set $\theta=0.6667$ (which corresponds to the Galerkin

Table 4
Mix proportions in concrete

(kg/m^3)	
Cement	323
Water	142
Sand 0/4	721
Fine gravel 6/14	1157

Table 6
Idealized composition of 1 m^3 of hydrated cement paste

Hydrates	mol/m^3 of cement paste
AFm	570
Hexa	290
CH	4350
C–S–H	4290

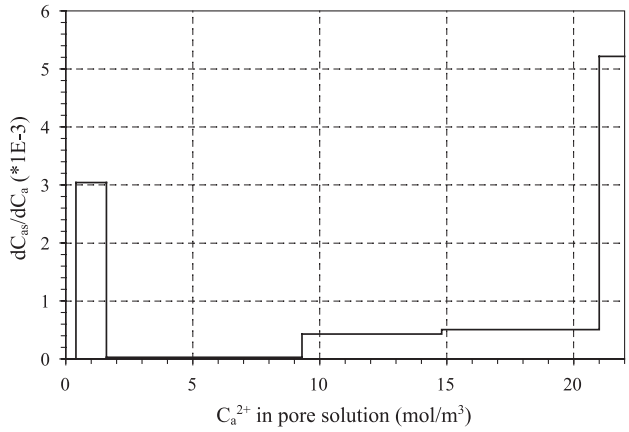

Fig. 2. Dissolved calcium source used in the calcium mass conservation equation.

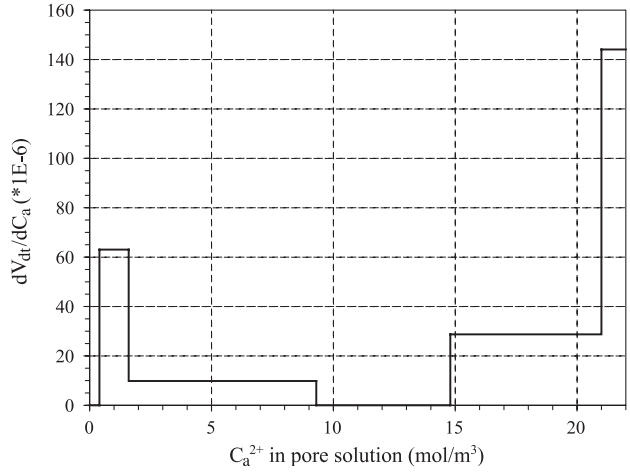

Fig. 4. Source term corresponding to the volume of dissolved hydrates.

method). The coefficients appearing in the algebraic equations, which depend upon the unknown variables, are assessed in the time domain $[t_n, t_{n+1}]$, by making use of the converged solution of the two previous steps at t_n and t_{n-1}; the value of the coefficient K_{β_n} is given by:

$$K_{\beta_n} = (1+\beta)K_{t_n} - \beta\, K_{t_{n-1}} \qquad \text{with } 0 \le \beta \le 1. \tag{44}$$

For the applications, the value β=.5 has been chosen.

4.2. Simulation of an accelerated carbonation test

4.2.1. Boundary conditions

The boundary conditions of the simulated structure are defined by:

- Flux set to zero for the three species at one extremity, corresponding to symmetry conditions, and describing the conditions which prevail in the core of the structure,
- Prescribed values of both carbon dioxide and saturation degree, and flux of calcium ions set to zero at the other extremity, representing the conditions at the surface exposed to external aggression.

4.2.2. Chemical properties

As an example, we have simulated an accelerated carbonation test on high-performance concrete specimen carried out by Miragliotta [18]. The cement used is a CPA CEM I 52.5 R; its average chemical composition is given in Table 3.

Aggregates used are sand 0/4 mm of real density 2550 kg/m^3, and fine crushed gravel 6/14 mm of real density 2600 kg/m^3; these aggregates are inert with regard to the carbonation process. The concrete composition is described in Table 4 and leads to a compressive strength at 28 days of 65.9 MPa. The water–cement ratio calculated from Table 4 is equal to 0.43 and leads to the cement paste chemical composition given in Table 5. Using Eq. (39), we obtain the

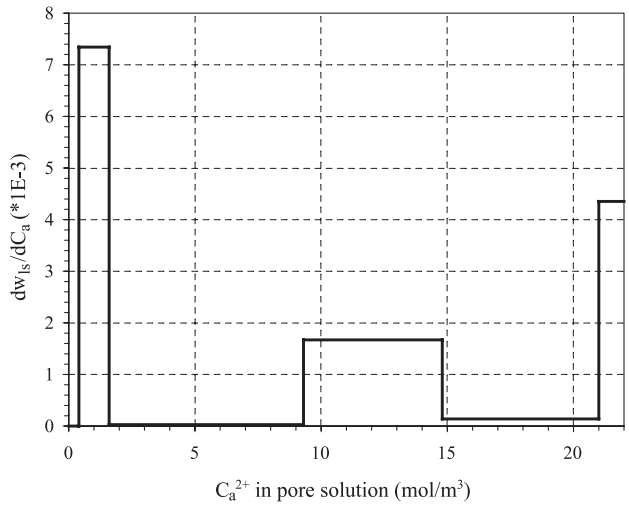

Fig. 3. Released water source term for dissolved hydrates.

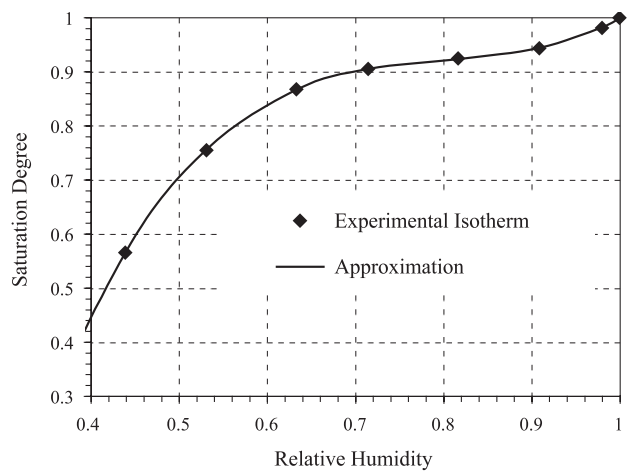

Fig. 5. Experimental and approximated desorption isotherm.

idealized hydrated cement paste composition shown in Table 6.

According to Table 2, and with the values calculated in Table 6, the source term dC_{aS}/dC_a used in the calcium mass conservation in Eq. (36) and defined per m^3 of cement paste is shown on Fig. 2. Furthermore, the evolutions of released water due to hydrate dissolution and volume of dissolved hydrates, corresponding to the term $d\omega_{lS}/dC_a$ and dV_{dt}/dC_a in Eq (23), both defined in Table 2, are depicted in Figs. 3 and 4 for 1 m^3 of cement paste, respectively.

The source terms shown on Figs. 2, 3 and 4 are calculated for 1 m^3 of cement paste, but since, in our case, the concrete contains 25% of hydrated cement paste, these source terms must be reduced by this rate before being transposed in the mass conservation equations for concrete.

4.2.3. Physical properties

The relation between the relative humidity h_r and the saturation degree S_r is given by the inversion of the desorption isotherm expression adopted to reproduce the experimental results in the range $h_r = 60\%$ to 100% taken from Ref. [8]. This expression is given in the following simplified form:

$$S_r = Ah_r^3 + Bh_r^2 + Ch_r + D. \quad (45)$$

The coefficients appearing in Eq. (45) are fitted to the values: $A = 6.43$, $B = -15.46$, $C = 12.52$ and $D = -2.50$ (see Fig. 5). The following numerical values are used for performing the simulations, some of them drawn from Ref.[18] when available: $\phi = 0.094$, $K\rho_{lg}/\eta = 1\times10^{-15}$ m/s, $V_{CaCO_3} = 36.9\times10^{-6}$ m^3/mol, $D_{\bar{c}} = 8\times10^{-7}$ m^2/s. The boundary conditions are $p_{\bar{c}\ max} = 50$ kPa, $h_r = 65\%$ and $C_a = 0$, whereas the initial conditions are set to $p_{\bar{c}} = 0$, $h_r = 94\%$ and $C_a = 22$ mol/m^3, with the length of the concrete specimen equal to 5 cm.

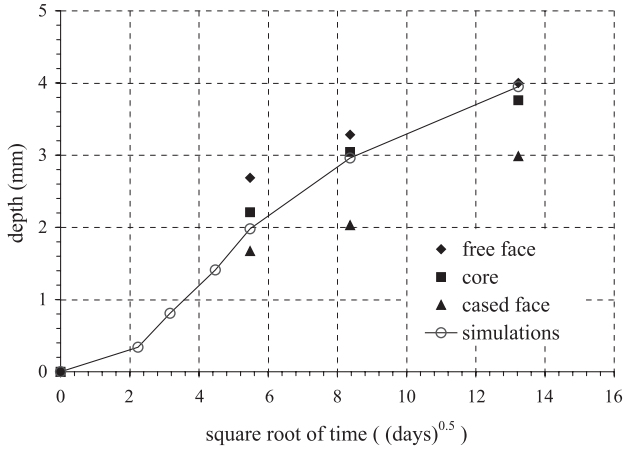

Fig. 7. Carbonation depth versus square root of time.

4.2.4. Numerical results

Fig. 6 presents the calcium concentration profiles numerically obtained at different times between 5 and 175 days. The carbonated zones correspond to the zones where the calcium concentration is closed to zero. It can be observed that in the first stage (5 to 70 days), the carbonation front propagation is mainly governed by CO_2 diffusion in the carbonated zone. After this stage, the concentration profile is modified due to a progressive filling of the porosity by calcite, as illustrated by Fig. 8. The porosity filling occurs progressively because it is conditioned by the quantity of dissolved calcium arriving from the sound zone, this quantity being essentially governed by diffusion processes.

The decreasing rate of the carbonation front propagation induced by the progressive porosity filling can also be observed on Fig. 7, where numerical prediction, as well as experimental data of the carbonation depth versus time, shows a propagation rate lower than the one obtained with a constant diffusion coefficient (i.e., proportional to the square

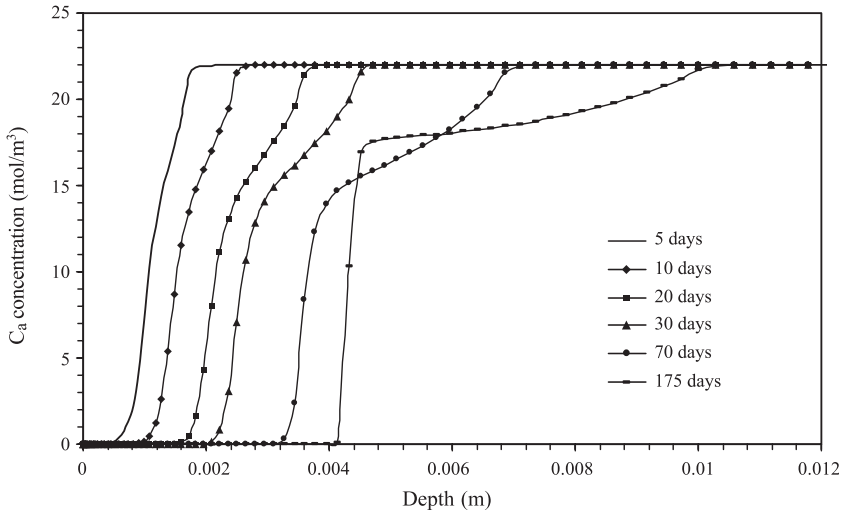

Fig. 6. Calcium concentration in porosity water versus depth for different times between 5 and 175 days.

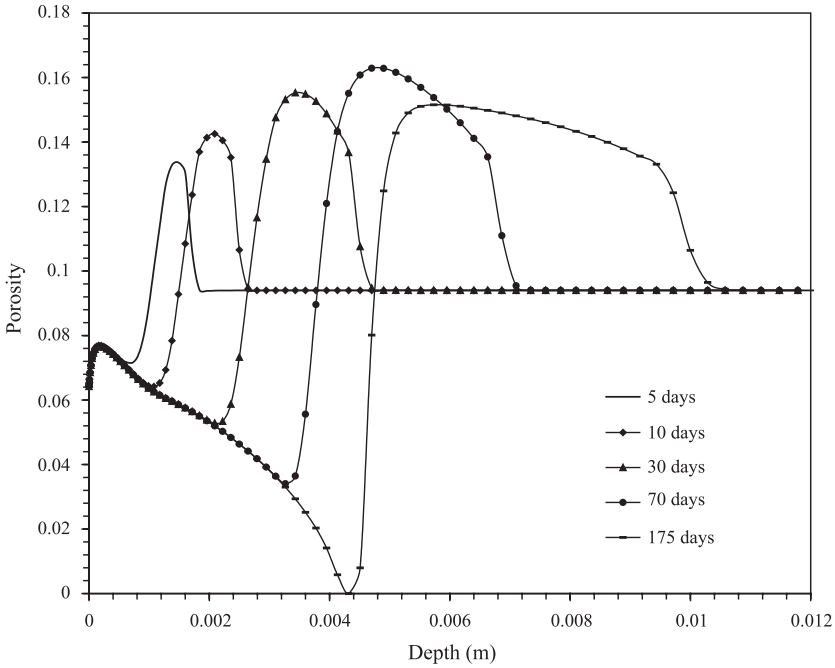

Fig. 8. Simulated porosity profiles for different time between 5 and 175 days.

root of time). It can also be remarked on Fig. 6 the slight decrease of calcium concentration behind the carbonation front, which means that dissolution process (essentially reduced to the portlandite) occurs in this zone.

In the Miragliota study [18], the specimens subjected to carbonation were extracted from different parts of a same concrete block (cased face, free face without any cure or core of the block), aiming at analyzing the effects of different porosities on the carbonation kinetic. However, numerical simulations presented here have been carried out only on the concrete corresponding to the core of the concrete block, where the initial porosity is assumed to be homogeneous. In this configuration, the model appears to correctly reproduce experimental results.

Fig. 8 shows the porosity profiles obtained numerically for different times ranging from 5 to 175 days; the face exposed to atmospheric carbonation is located at depth 0. The progressive filling of the porosity in the carbonated zone appears clearly. We can notice that this filling increases with the carbonation front progression. Simulta-

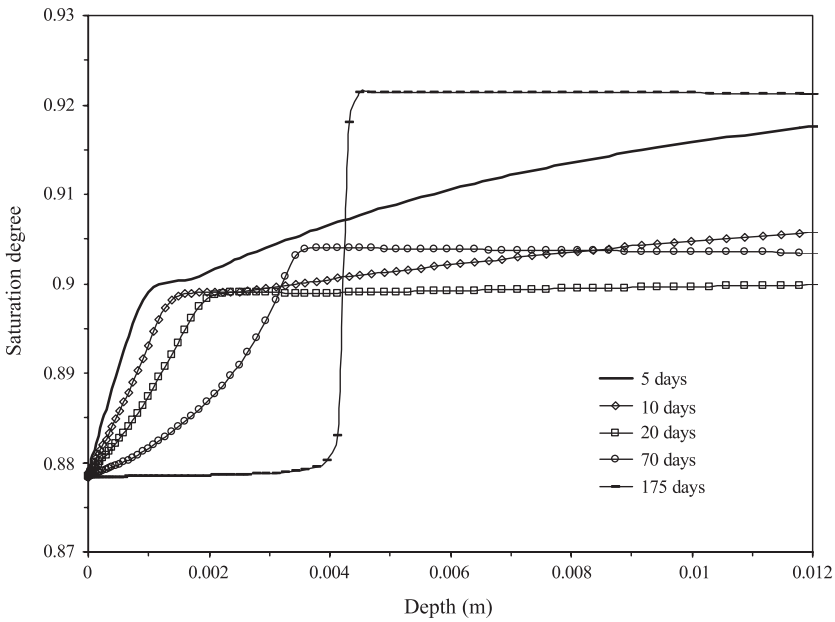

Fig. 9. Saturation degree profiles for different time between 5 and 175 days.

neously, an increase of the porosity occurs just ahead of the carbonation front, which results from the calcium leaching (diffusion) from the sound zone to the carbonated zone due to the calcium concentration gradient. These observations permit to conclude that the possibility of a total porosity filling depends not only on the quantity of calcium locally available in the zone where carbonation occurs, but also on the calcium dissolved in the pore solution and transported by convection and diffusion from the sound zone. The CH quantity, alkali contents, and transfer properties are of major importance regarding the porosity-filling phenomenon.

Fig. 9 shows the numerical saturation degree profiles at different times. Up to 20 days, the saturation degree gradient is positive from the exposed face to the sound zone; water transfer then occurs from the inside of the specimen to the outside. Later than 20 days, it can be observed an inversion of the saturation degree gradient behind the carbonation front due to the combined effect of the progressive porosity filling (conducting to increase the saturation degree in the carbonated zone at constant water mass) and the released water consecutive to the dissolution process. At 175 days the water transfer toward the external surface is stopped because of the quasi-total porosity filling, as can be seen on Fig. 8. The saturation degree reaches independent values on each side of the zone, where the porosity is reduced to nearly 0. In the carbonated zone, this value is conditioned by the external relative humidity boundary condition, whereas in the sound zone the residual total quantity of liquid water progressively homogenizes.

5. Conclusion

The approach developed in this paper for describing the carbonation of concrete takes into account simultaneously carbon dioxyde, dissolved calcium and liquid water transfers. The coupled partial differential equations set is obtained by using the classical mass balance principle where both diffusive and convective transfers are considered. Chemical equilibriums are introduced using a simplified chemical zoning on idealized hydrated cement paste. This method allows to estimate the source or sink terms used in mass balance equations according to the chemical composition of cement. Diffusion coefficient and gaz and water permeabilities are affected by the dissolution or the precipitation phenomena and by the saturation degree variation. The functions introduced for linking the porosity and the saturation degree variations to the transfer coefficients are fitted on experimental data or taken from literature; however, the empirical aspect of some of these functions would deserve a deepened development. In its current version, the model gives interesting results, which permit to improve the global comprehension of the carbonation processes and constitutes a powerful prediction tool. Indeed, it allows in particular to consider any initial nonhomogeneous saturation degree and porosity profiles and computes their evolution during carbonation.

The simulation of an accelerated carbonation test and its comparison to experimental data shows an acceptable agreement in terms of carbonation depth. Moreover, the numerical results point out some aspects, which turn out to be of importance with regard to the carbonation mechanisms. The main aspects are the progressive filling of the porous space in the carbonated zone (which has, in turn, a direct impact on the moisture, carbon dioxide and calcium transfers properties) and the quantity of solid calcium available for dissolution and calcite precipitation.

Acknowledgements

Fruitful discussions and financial support from the French national agency for nuclear waste management (ANDRA) is gratefully acknowledged.

References

[1] A.V. Saetta, B.A. Schrefler, R.V. Vitaliani, 2-D model for carbonation and moisture /heat flow in porous materials, Cem. Concr. Res. 25 (8) (1995) 1703–1712.
[2] B.F. Johannesson, Nonlinear transient phenomena in porous media with special regard to concrete and durability, Adv. Cem. Based Mater. 6 (1997) 71–75.
[3] A.V. Saetta, B.A. Schrefler, R.V. Vitaliani, The carbonation of concrete and the mechanism of moisture, heat and carbon dioxide flow through porous materials, Cem. Concr. Res. 23 (4) (1993) 761–772.
[4] S.K. Roy, K.B. Poh, D.O. Northwood, Durability of concrete—accelerated carbonation and weathering studies, Build. Environ. 34 (1999) 597–606.
[5] K. Van Balen, D. Van Gemert, Modeling lime mortar carbonation, Mat. Struct. 27 (1994) 393–398.
[6] L. Ying-Yu, W. Qui-Dong, The mechanism of carbonation of mortars and the dependence on carbonation on pore structure, Int. Conf. on Concrete Durability, vol. 2, ACI, Detroit, MI, 1987, pp. 1915–1943.
[7] V.G. Papadakis, C.G. Vayenas, M.N. Fardis, Fundamental modeling and experimental investigation of concrete carbonation, ACI Mater. J. 88 (4) (1991) 363–373.
[8] V. Baroghel-Bouny, M. Mainguy, T. Lassabatère, O. Coussy, Characterization and identification of equilibrium and transfer moisture properties for ordinary and high-performance cementitious materials, Cem. Concr. Res. 29 (1999) 1225–1238.
[9] M. Mainguy, O. Coussy, V. Baroghel-Bouny, Role of air pressure in drying of weakly permeable materials, J. Eng. Mech. 127 (6) (2001) 582–592.
[10] P. Faucon, F. Adenot, J.F. Jacquinot, J.C. Petit, R. Cabrillac, M. Jorda, Long-term behaviour of cement pastes used for nuclear waste disposal: review of physico–chemical mechanisms of water degradation, Cem. Concr. Res. 28 (6) (1998) 847–857.
[11] F. Adenot, Durabilité des bétons: Caractérisation et modélisation des processus physiques et chimiques de dégradation du ciment. PhD thesis of the University of Orléans 1992 (in French).
[12] O. Coussy, Mechanics of Porous Continua, Wiley, Chichester, 1995.
[13] M. Mainguy, C. Tognazzi, J.M. Torrenti, F. Adenot, Modelling of leaching in pure cement paste and mortar, Cem. Concr. Res. 30 (2000) 83–90.
[14] Z.P. Bazant, L.J. Najjar, Nonlinear water diffusion in nonsaturated concrete, Mat. Struct. 5 (25) (1972) 3–20.

[15] M.T. van Genuchten, A closed-form equation for predicting the hydraulic conductivity of unsaturated soils, Soil Sci. Soc. Am. Proc. 44 (1980) 892–898.
[16] P.W. Atkins, Physical Chemistry, Sixth edition, Oxford Univ. Press, Oxford, 1998.
[17] G. Verbeck, Carbonation of hydrated Portland cement, ASTM Spec. Publ. 205 (1958) 17–36.
[18] R. Miragliotta, Modélisation des processus physico-chimiques de la carbonatation des bétons préfabriqués—Prise en compte des effets de parois. PhD thesis of the University of la Rochelle, 2000 (in French).
[19] S.R. de Groot, P. Mazur, Non-Equilibrium Thermodynamics, Dover Publications, New York, 1984.
[20] R.J. Millington, Gas diffusion in porous media, Science 130 (1959) 100–102.
[21] A.E. Adenakan, T. Patzek, K. Pruess, Modeling of multiphase transport of multicomponent organic contaminants and heat in the subsurface: numerical model formulation, Water Resour. Res. 29 (11) (1993) 3722–3740.
[22] C. Tognazzi, Couplage fissuration—Dégradation chimique dansles matériaux cimentaires: caractérisation et modélisation, thèse de doctorat de l'Institut National des sciences Appliquées de Toulouse, soutenue le 11 décembre, 1998 (in French).
[23] H.F.W. Taylor, Cement Chemistry, Second edition, Thomas Telford, London, 1997.
[24] E. Samson, J. Marchand, J.J. Beaudoin, Modeling the influence of chemical reactions on the mechanisms of ionic transport in porous materials. An overview, Cem. Concr. Res. 30 (2000) 1895–1902.
[25] K. Fuji, W. Kondo, Heterogeneous equilibrium of calcium silicate hydrate in water at 30 °C, J. Chem. Soc., Dalton Trans. (1981) 645–651.